04-004

THREE-DIMENSIONAL HYDRODYNAMIC MODELING IN THE CONFLUENCE OF YANUNCAY AND TARQUI RIVERS, PROVINCE OF AZUAY-ECUADOR

Ochoa García, Santiago Aurelio [(1)]; Matovelle Bustos, Carlos Marcelo [(1)]; Córdova González, Nelson Federico [(1)]; Maldonado Noboa, César Humberto [(1)]

[(1)] Universidad Católica de Cuenca

The experimental and numerical characterization of flow variables in channels, rivers, and coastal areas is still a challenge for the research branches related to hydraulic engineering; this is due to the complicated physical interaction of the hydrodynamic processes that occur in natural flows. It highlights the need to study complex phenomena where the hypothesis of unidimensionality is too far from reality, leading to proposal projects for the development and application of appropriate numerical methods to evaluate hydrodynamic flow's conditions that flow through populated areas of importance, as is the case of the confluence of the Yanuncay River with the Tarqui River located south of the city of Cuenca, capital of the province of Azuay in the Republic of Ecuador. In this work, simulations have been carried out on the confluence of Yanuncay and Tarqui rivers using the DELFT3D model, we have identified the typical characteristics of a confluence such as highly erosive cut and separation layers, stagnation zones and turbulent mixtures, flow acceleration and reestablishment zones. This has provided a tool to evaluate the vulnerability of confluence flows in mountain rivers in the Ecuadorian Andes.

Keywords: three-dimensional hydrodynamics; confluence; mountain rivers

MODELACIÓN HIDRODINÁMICA TRIDIMENSIONAL DE LA CONFLUENCIA DE LOS RÍOS YANUNCAY Y TARQUI, EN LA PROVINCIA DEL AZUAY-ECUADOR

La caracterización experimental y numérica de las variables de flujo en canales, ríos y áreas costeras son todavía un desafío para las ramas de investigación relacionadas a la ingeniería hidráulica; esto debido a la complicada interacción física de los procesos del hidrodinámicos que ocurren en los escurrimientos naturales. Se destaca la necesidad de estudiar fenómenos complejos en donde la hipótesis de unidimensionalidad se aleja demasiado de la realidad, conduciendo a plantear proyectos para el desarrollo y aplicación de métodos numéricos adecuados para evaluar condiciones hidrodinámicas en flujos que escurren por sectores poblados de importancia, como es el caso de la confluencia del río Yanuncay con el río Tarqui ubicado al sur de la ciudad de Cuenca, capital de la provincia del Azuay de la república del Ecuador. En este trabajo se han realizado simulaciones en la confluencia de los ríos Yanuncay y Tarqui utilizando el modelo DELFT3D, se han identificado las características típicas de una confluencia tales como capas de corte y separación altamente erosivas, zonas de estancamiento y mezclas turbulentas, zonas de aceleración y restablecimiento del flujo. Esto ha proporcionado una herramienta para evaluar la vulnerabilidad de los flujos de confluencia en los ríos de montaña de los Andes ecuatorianos.

Palabras clave: hidrodinámica tridimensional; confluencia; ríos de montaña

Agradecimientos: Se agradece el financiamiento de la Universidad Católica de Cuenca dentro de los Proyectos de Investigación (PICODS21-33) e Investigación Formativa (PIFCV22-04), gracias a esta colaboración es posible obtener los resultados presentados y continuar con la

1. Introduction

A common phenomenon in natural rivers is open-channel confluences that play an important role in hydraulic engineering works due to the complex interaction between the main channel and tributary flows (Shaheed et al, 2022). A large number of numerical studies have been undertaken to explain the characteristics of river confluences (Taylor, 1944; Mosley, 1976; Best, 1987; Ashmore and Parker, 1983; Hager, 1989; Biron et al, 1996; Gurram et al, 1997; Ramamurthy and Zhu, 1997; Huang et al, 2002; Behrangi et al, 2004; Shakibainia et al, 2010; Thanh et al, 2010; Constantinescu et al, 2014; Cedillo-Galarza et al, 2021; Shaheed et al, 2022).

The evaluation, simulation, and characterization of river confluences is a subject that has generated considerable interest in the scientific community both from the hydrodynamic point of view and for the evaluation of water quality. The knowledge obtained has allowed the development of several models of flow dynamics in different types of confluences. Mosley (1976) and Best (1986) developed conceptual models of flow structures for symmetrical confluences. Best (1987) generated a model for asymmetric confluences that has been widely adopted and recognizes the following hydrodynamic regions:

1. Flow stagnation zone immediately downstream of the confluence top.
2. A shear layer and a mixing interface in the combination of the two flows. The shear layer has been defined as a zone of intense turbulence due to differences in the amount of motion between the confluent flows (Rhoads and Sukhodolov, 2008), and has observed as a narrow strip within the vertically oriented flow cross section, perpendicular to the channel bottom, and where high levels of turbulent kinetic energy has recorded.
3. Flow separation downstream of the stagnation zone and on the downstream faces of the tributary steps at the mouth of the confluence.
4. Flow acceleration reaches its maximum velocity when the two tributaries meet.
5. Flow recovery downstream of the confluence.
6. Secondary currents in the convergence zone of the flow will be associated with its curvature.

The characteristics of the described zones depend on the geometry of the confluence, the angle between the converging flows, the ratio of moments, and the morphology of the bed (Díaz-Lozada, 2019). The complex hydrodynamics of these flows in natural streams also significantly affect the mixing processes and cause the equations developed in the literature to present significant shortcomings in some cases because they have developed in laboratories or for natural streams with different characteristics from those of the system proposed. Therefore, the scientific importance of applying innovative numerical techniques for the simulation and evaluation of confluences in mountain or torrential rivers has emphasized.

This paper evaluates the hydrodynamic characteristics of a confluence formed by mountain rivers in the Ecuadorian Andes. The application domain had located in the urban area of the city of Cuenca, at the confluence of the Yanuncay and Tarqui rivers. The morphological characteristics of mountain rivers modify hydrodynamic conditions regarding low-gradient rivers (Cedillo-Galarza et al., 2021), thus highlighting the scientific need to evaluate

hydrodynamics at a confluence in the southern Ecuadorian Andes through the application of numerical models.

2. Methodology

2.1 Application Domain

The city of Cuenca, located in the south of the Republic of Ecuador, is third in political and economic importance in the country after the cities of Quito and Guayaquil. Cuenca is known for the flow of its four rivers (Tomebamba, Yanuncay, Tarqui and Machángara), which have been protagonists in the continuous development of the southern region of Ecuador. These four rivers form part of the tributaries in the Paute River basin, where important hydroelectric projects are located, generating about 30% of Ecuador's hydroelectric energy (CELEC E.P., 2023). Because of their mountainous relief, the tributaries of the upper Paute River basin could be classified as mountain rivers, due to their steep slopes and large hillsides that generate flash floods with risks associated with the overflowing of riverbeds and flooding in residential areas of the city. In this work, a hydrodynamic analysis of the confluence of the Yanuncay and Tarqui rivers located in the south of the city of Cuenca has been proposed (Figure 1):

Figure 1: Location of the Application Area.

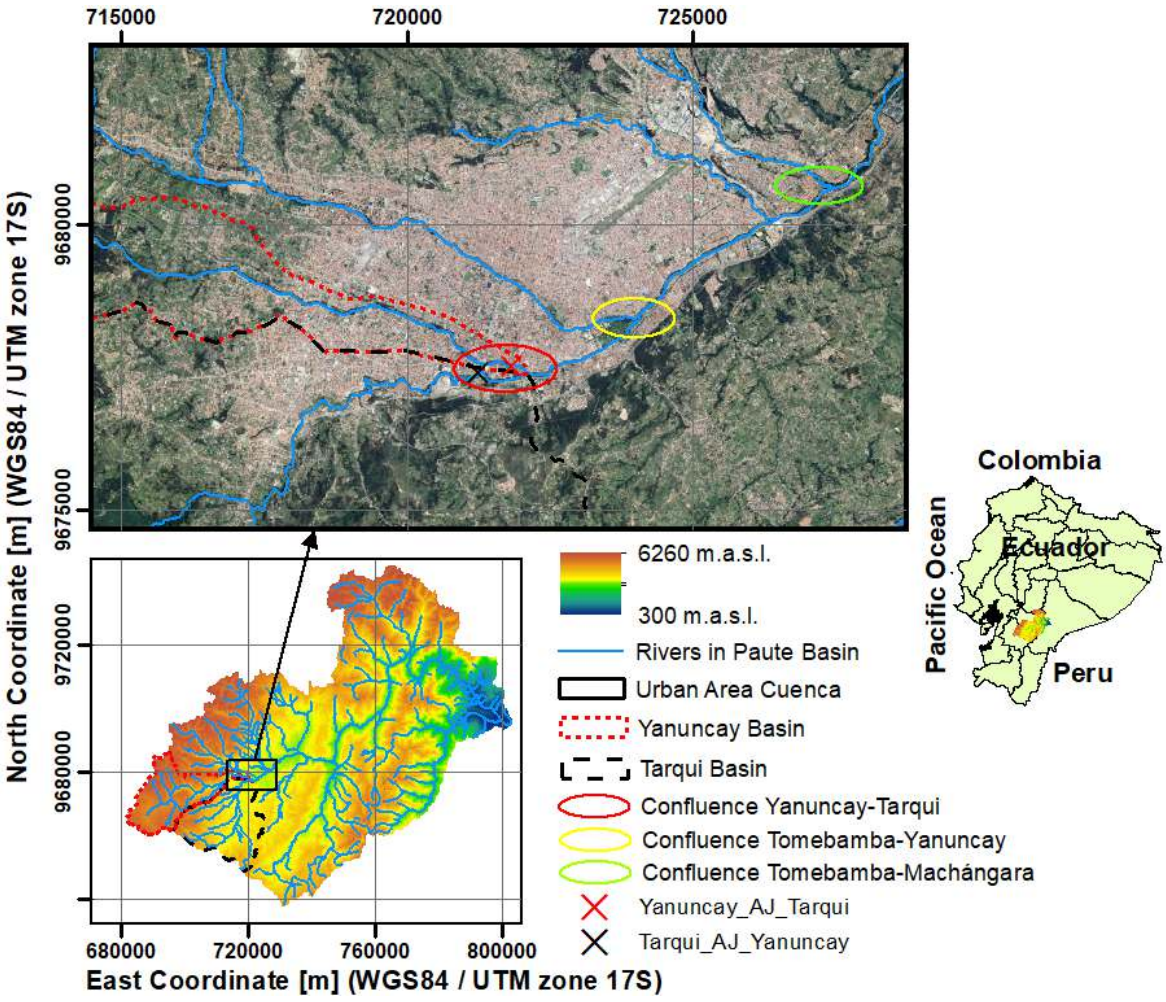

The flow of four rivers through the city of Cuenca generates three important confluences within the urban area (Figure 1), in order of occurrence: 1) The junction of the Yanuncay river with the Tarqui river, where the river formed has the name of Yanuncay; 2) The junction of the

Tomebamba river with the Yanuncay river, where the river formed has the name of Tomebamba; 3) The junction of the Tomebamba river with the Machángara river, where the river formed is called the Cuenca river. In Table 1 we present the main physiographic characteristics of the contributing basins at the confluence of the Yanuncay and Tarqui rivers.

Table 1. Physiographic Characteristics of the Contributing Basins.

Basin	Area (km^2)	Perimeter (km)	Length (km)	River Length (km)	Average Slope (%)
Yanuncay	417.8	148	43.7	45.2	23.2
Tarqui	476.6	110.9	27.2	23.5	23.6

To characterize the hydrological behavior of the contributing basins it is necessary to evaluate their land use and vegetation cover. Based on available information from the “Sistema Nacional de Información de Tierras Rurales e Infraestructura Tecnológica” (SIGTIERRAS, 2023) database, the land use area of the Yanuncay and Tarqui river basins has been estimated (Table 2).

Table 2. Land Use Area in the Contributing Watersheds (km^2).

Basin	Forest Natural Forest and Vegetation Native	Superficial Water	Paramo	Crops and Pasture	Soil uncovered, settlements and roads	Anthropic Vegetation
Tarqui	102.9	0.8	70.8	227.7	45.9	28.5
Yanuncay	56.8	3.8	152.9	159.7	38.9	5.7

The Yanuncay river basin has a paramo area approximately twice as big as the Tarqui river basin. In contrast, the Tarqui river basin has dominated by natural/anthropic vegetation and agricultural areas compared to the Yanuncay river basin. The Paramo ecosystem is the most important source of water in the Andean highlands (Minaya Maldonado, 2017), contributing to or affecting water storage, flow regulation, and biodiversity (Vuille, 2013). In this sense, even though the Yanuncay river basin has a smaller contributing surface area than the Tarqui river basin, the average flows of the Yanuncay river before the confluence are expected to be of greater magnitude than those of the Tarqui river.

2.2 Hydrological Information

To estimate the flows of the tributaries considered, the information from the hydrological stations installed with level sensors that are operated by the “Empresa Pública Municipal de Telecomunicaciones, Agua Potable y Alcantarillado de Cuenca” (ETAPA E.P., 2023) will be analyzed. The "Yanuncay_AJ_Tarqui" and "Tarqui_AJ_Yanuncay" stations measure the water level in the Yanuncay and Tarqui rivers in sections upstream of their confluence (Figure 1). Based on the discharge curves obtained from liquid gauging data on the control sections, the flow rate is related to the mean monitored level with a time step of 5 minutes. The discharge

curves represent a potential relationship between the height of the river water at a point in the control section and the volume of water flow per unit of time.

$$Q = (7.63569 * 10^{-6}) * (H - 26)^{3.01851} \quad (1)$$

$$Q = (1.45966 * 10^{-6}) * (H - 20)^{3.3435} \quad (2)$$

The Eq. 1 and Eq. 2, Q represents the flow in m^3/s estimated with the height H (centimeters). These represent the discharge curves in the control sections of the Yanuncay and Tarqui rivers before the confluence, respectively. In a cross-section of a natural channel, the exact relationship between water level (H) and discharge (Q) must be determined through flow measurements. The application of obtained discharge curves (Eq. 1 and Eq. 2) is more realistic than relying solely on deterministic physical relationships to estimate the flow rate. In Figure 2 we showed the time series of levels and flows monitored in the control sections.

Figure 2: Hydrological Observing Data Upstream of the Yanuncay-Tarqui Confluence.

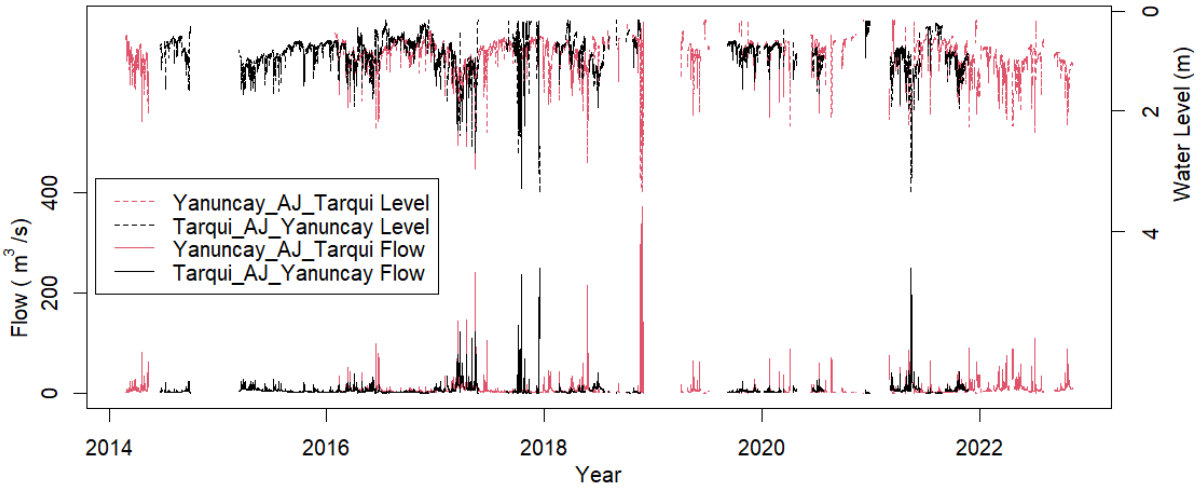

The information monitored for the flow analysis in the Yanuncay and Tarqui rivers was from February 2014 to November 2022, with an hourly time step. The estimated average flow in the Yanuncay River before the confluence is 7.01 m3/s and in the Tarqui River is 5.61 m3/s. The maximum flows monitored during the period corresponded to 371.12 m3/s in the Yanuncay River and 249.45 m3/s in the Tarqui River. For the hydrodynamic modelling the maximum events monitored by the level sensors have been considered. In Figure 3 we showed those events.

Figure 3: Peak Flows: (a) Yanuncay_AJ_Tarqui, (b) Tarqui_AJ_Yanuncay.

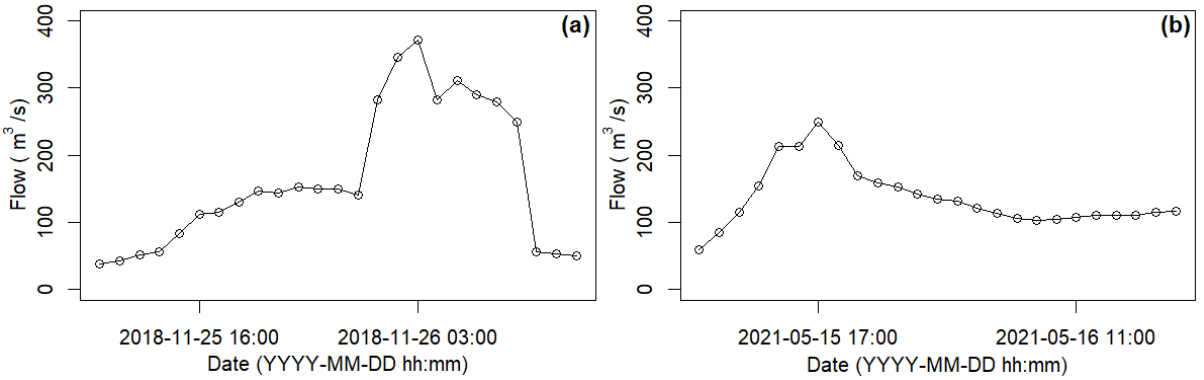

The flow hydrographs presented in Figure 3 have a duration of 24 hours. The Yanuncay river event was monitored starting November 25, 2018, with an initial flow of 38.18 m^3/s and with a

total flow volume of 14.68 Hm^3. The Tarqui River event was monitored as of May 15, 2021, with an initial flow of 58.83 m^3/s and with a total flow volume of 12.26 Hm^3. The events described will be the flows considered in the hydrodynamic numerical model implemented at the confluence.

2.3 Delft3D Model

The hydrodynamic model (FLOW Module) of Delft3D solves the Navier-Stokes equations on a curvilinear mesh, assuming the Boussinesq hypotheses. The set of partial differential equations in combination with an appropriate set of initial and boundary conditions is solved on a finite difference mesh using the Reynolds Averaged Navier Stokes (RANS) method. Turbulent fluctuations are included in the model through Reynolds stresses, defined through the turbulence closure model, in this case, the two-equation *k-ε* closure model (Uittenbogaard et al, 1992).

The numerical solution of the hydrodynamic equations requires the spatial (horizontal) discretization of the study area. For this purpose, a mesh with an appropriate number of cells is superimposed on the calculation domain, depending on the detail required by the type of problem to be studied (waves, currents, river inflow) and by the proximity to the areas of great interest (river mouth, water intake point) (Gyssels et al, 2013). The depth-averaged continuity equation solved by Delft3D is given by Eq. 3.

$$\frac{\partial \varsigma}{\partial t} + \frac{1}{\sqrt{G_{\xi\xi}}\sqrt{G_{\eta\eta}}}\frac{\partial\left((d+\varsigma)U\sqrt{G_{\eta\eta}}\right)}{\partial \xi} + \frac{1}{\sqrt{G_{\xi\xi}}\sqrt{G_{\eta\eta}}}\frac{\partial\left((d+\varsigma)V\sqrt{G_{\xi\xi}}\right)}{\partial \eta} = (d+\varsigma)Q \tag{3}$$

In Eq. 3, t represents the time variable, ξ and η represent the curvilinear coordinates in the plane, $\sqrt{G_{\xi\xi}}$ and $\sqrt{G_{\eta\eta}}$ represent the conversion factors from curvilinear coordinates to plane coordinates that depend on the radius of the earth and the location of the application, U and V represent the horizontal components of the depth-averaged velocity, Q represents the source term that considers the inflow or outflow of the system (Deltares, 2022).

The equations of quantity of motion for the horizontal flow directions (u, v), are given by:

$$\frac{\partial u}{\partial t} + \frac{u}{\sqrt{G_{\xi\xi}}}\frac{\partial u}{\partial \xi} + \frac{v}{\sqrt{G_{\eta\eta}}}\frac{\partial u}{\partial \eta} + \frac{w}{d+\varsigma}\frac{\partial u}{\partial \sigma} - \frac{v^2}{\sqrt{G_{\xi\xi}}\sqrt{G_{\eta\eta}}}\frac{\partial\sqrt{G_{\eta\eta}}}{\partial \xi} + \frac{uv}{\sqrt{G_{\xi\xi}}\sqrt{G_{\eta\eta}}}\frac{\partial\sqrt{G_{\xi\xi}}}{\partial \eta} - fv = -\frac{1}{\rho_0\sqrt{G_{\xi\xi}}}P_\xi + F_\xi + \\ + \frac{1}{(d+\varsigma)^2}\frac{\partial}{\partial \sigma}\left(\nu_V\frac{\partial u}{\partial \sigma}\right) + M_\xi \tag{4}$$

$$\frac{\partial v}{\partial t} + \frac{u}{\sqrt{G_{\xi\xi}}}\frac{\partial v}{\partial \xi} + \frac{v}{\sqrt{G_{\eta\eta}}}\frac{\partial v}{\partial \eta} + \frac{w}{d+\varsigma}\frac{\partial v}{\partial \sigma} - \frac{uv}{\sqrt{G_{\xi\xi}}\sqrt{G_{\eta\eta}}}\frac{\partial\sqrt{G_{\eta\eta}}}{\partial \xi} + \frac{u^2}{\sqrt{G_{\xi\xi}}\sqrt{G_{\eta\eta}}}\frac{\partial\sqrt{G_{\xi\xi}}}{\partial \eta} + fu = -\frac{1}{\rho_0\sqrt{G_{\eta\eta}}}P_\eta + F_\eta + \\ + \frac{1}{(d+\varsigma)^2}\frac{\partial}{\partial \sigma}\left(\nu_V\frac{\partial v}{\partial \sigma}\right) + M_\eta \tag{5}$$

In Eq. 4 and Eq. 5, (u, v, w) represent the 3 velocity components along the Cartesian axes, f represents the Coriolis parameter that depends on the rotational velocity of the earth, ρ_0 represents the density of water, P_ξ and P_η represent the hydrostatic pressure components in the plane, F_ξ and F_η represent the turbulent flow components in the plane, ν_V represents the viscosity of the flow, M_ξ and M_η represent the source term components of momentum flows in the plane (Deltares, 2022).

For the solution of the third equation of quantity of motion, the vertical discretization in σ coordinates must be considered, leaving the equation of quantity of motion in the w vertical direction of the flow as follows:

$$\frac{\partial \varsigma}{\partial t} + \frac{1}{\sqrt{G_{\xi\xi}}\sqrt{G_{\eta\eta}}}\frac{\partial\left((d+\varsigma)u\sqrt{G_{\eta\eta}}\right)}{\partial \xi} + \frac{1}{\sqrt{G_{\xi\xi}}\sqrt{G_{\eta\eta}}}\frac{\partial\left((d+\varsigma)v\sqrt{G_{\xi\xi}}\right)}{\partial \eta} + \frac{\partial w}{\partial \sigma} = (d+\varsigma)(q_{in} - q_{out}) \quad (6)$$

In Eq. 6, q_{in} and q_{out} represent local sources and sinks per unit volume (Deltares, 2022).

Para la solución de las ecuaciones presentadas, el número de capas en la vertical fue constante para toda la zona de estudio. La integración temporal utilizada por el esquema de solución numérica (método cíclico) se ha basado en el método ADI (Alternating Direction Implicit). Este esquema no impone restricciones al intervalo temporal de cálculo.

For the time-dependent discretization of the equations, it must be taken into account that it is necessary to consider an appropriate time interval that can be determined by the type of problem according to the Courant-Friedrichs-Lewy number in order not to affect the quality of the solution (Deltares, 2022). The Courant-Friedrichs-Lewy number equation is given by:

$$CFL = \frac{\Delta t\sqrt{gH}}{\{\Delta x, \Delta y\}} < 10 \quad (7)$$

In Eq. 7, Δt is the time step, g represents the acceleration of gravity, H represents the mean flow stress, $\{\Delta x, \Delta y\}$ represent the characteristic value of the mesh dimensions in both directions (Deltares, 2022).

In section 2.4, the considerations made to apply Delft3D in the computational domain of the confluence of the Yanuncay and Tarqui rivers will be described.

2.4 Delft3D Implementation

According to Stelling (1984), a suitable solution method of the Reynolds-averaged Navier Stokes shallow water equations has to satisfy the following requirements: robustness, accuracy, suitability, stability, and computational efficiency. In the application for the computational domain, the explicit time integration of the shallow water equations on a rectangular grid was subjected to a time step condition of 0.005 seconds, complying with a Courant number of less than ten over the entire computational domain (Eq. 7).

The numerical mesh generated for the Delft3D modeling of the confluence of the Yanuncay and Tarqui rivers (Figure 4) consists of 9072 elements, with an average element size in the plane of approximately 2x2 meters. The vertical discretization was ten elements, with a constant thickness of 10% of the flow height.

To represent a Digital Terrain Model (DTM) suitable for hydrodynamic simulation (Figure 4) were surveyed 1630 points with equipment of precision (Total Station). In the topographic and bathymetric survey, 60 cross-sections were measured with an average length of 100 meters and spaced every 20 meters.

Figure 4: Computational Grid and DTM at the Yanuncay-Tarqui Confluence.

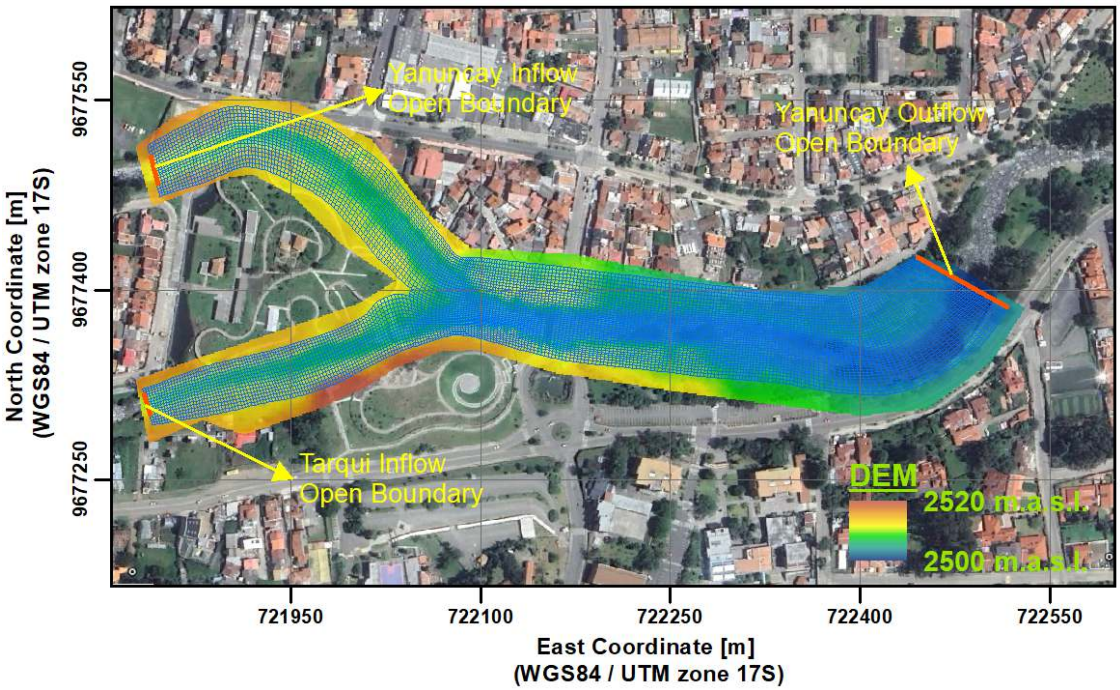

For the Delft3D simulation, three open boundaries were defined: the inflow through the Yanuncay River, the inflow through the Tarqui River, and the outflow boundary downstream of the confluence (Figure 4). The inflow boundaries were defined with the hydrographs for the events considered (Figure 3) and at the outflow boundaries, the water level was estimated for different flows by applying the definitions of Gradually Varying Flow and applying the Standard Passage Method downstream of the confluence (Chow, 1959).

The boundary conditions representing the flow resistance of solid boundaries were defined with Manning's friction coefficient (at the free surface the air resistance is neglected) (Deltares, 2022). Ibrahim & Abdel-Mageed (2014) emphasized the importance of a correct choice of Manning's friction coefficient with the flow results obtained in physical and numerical models with solid boundaries of different materials. The Manning's friction coefficient defined in the hydrodynamic modeling with Delft3D of the confluence of the Yanuncay and Tarqui rivers was 0.035 in the main channel and 0.065 in the flood banks, obtaining with these definitions numerical results that were close to reality.

3. Results Analysis

The Delft3D three-dimensional hydrodynamic model was applied to evaluate the hydraulic characteristics of a mountain river confluence located in the urban area of the city of Cuenca. For the proposed simulation, data obtained from two hydrological stations located upstream of the junction of the Yanuncay and Tarqui rivers were considered. The maximum 24-hour events of the series from February 2014 to November 2022 were simulated. To evaluate the typical characteristics of a confluence, the results will be analyzed in the time step in which the flow through the two rivers is similar, according to Figure 3, it corresponds to the time step 11 hours after the start of the event, which has a total flow at the confluence of 304.6 m^3/s contributed in equal parts by the two channels. With these considerations, Figure 5 were showed the results of the flow height in the confluence zone of the Yanuncay and Tarqui rivers.

Figure 5: Water Depth at the Yanuncay-Tarqui Confluence.

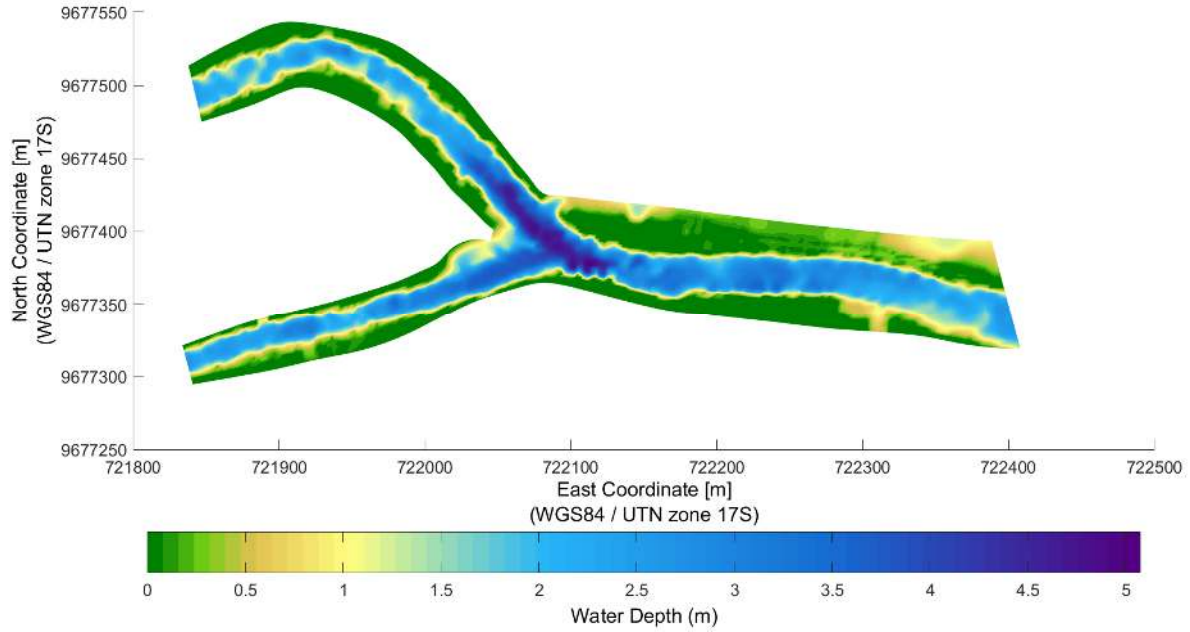

According to Figure 5 the maximum flow height of approximately five meters is present on the Yanuncay River in the confluence zone. The average flow height along the domain is approximately two meters. The flow heights are in the same order as the values observed in the hydrological stations considered to determine the flows contributed by the Yanuncay and Tarqui rivers (Figure 2). Overflow zones are identified on the left bank of the Yanuncay River from the junction with the Tarqui River. The evaluation of the kinetic characteristics of the confluence is carried out with the help of Figure 6, where the average flow velocities averaged over the vertical obtained with Delft3D are presented.

Figure 6: Depth Averaged Velocity at the Yanuncay-Tarqui Confluence.

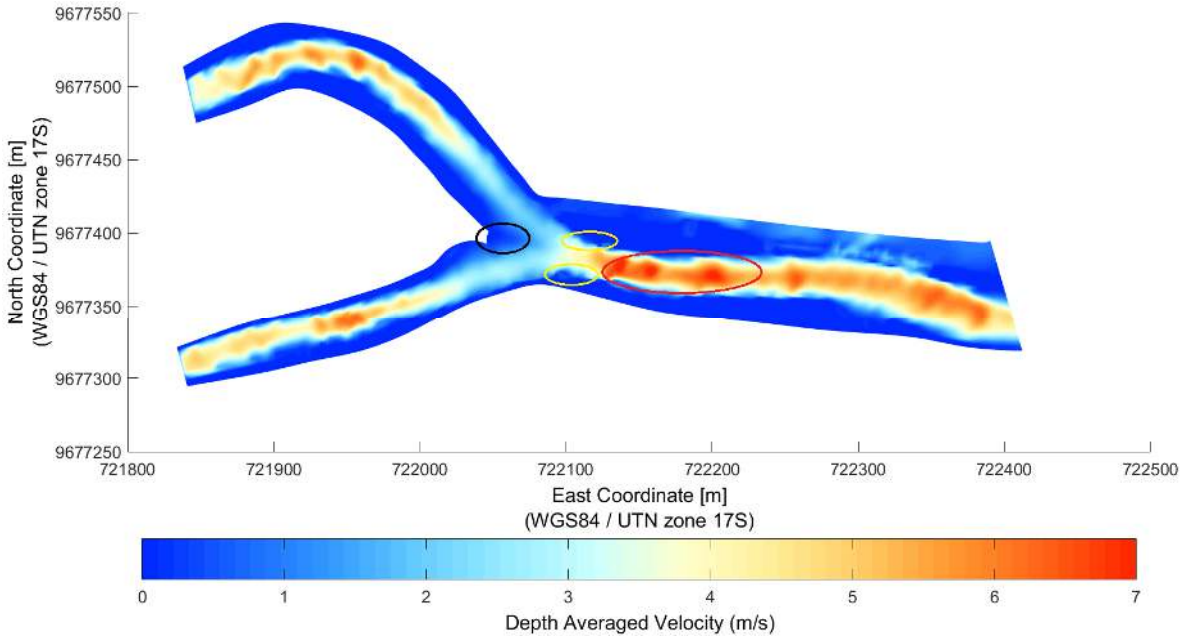

The analysis of the vertically averaged velocity results (Figure 6) shows the stagnation zone immediately downstream of the confluence tip, marked with black color. The shear and recirculation zones close to the banks downstream of the confluence can be identified (marked with yellow in Figure 6). Also, in Figure 6 the turbulent mixing zones with flow acceleration can be identified (marked with red). Downstream of the confluence the recovery of the flow can be observed with the gradual decrease of the velocity. The shear, mixing, and flow acceleration zones are associated with considerable magnitudes of shear stresses at the bottom that produce erosion at the flow boundaries. The shear stresses are directly proportional to the ratio of the flow velocity concerning its depth for the evaluation of the simulated dynamic characteristics at the confluence the results of the bottom shear stresses simulated with Delft3D are presented in Figure 7.

Figure 7: Bed Shear Stress at the Yanuncay-Tarqui Confluence.

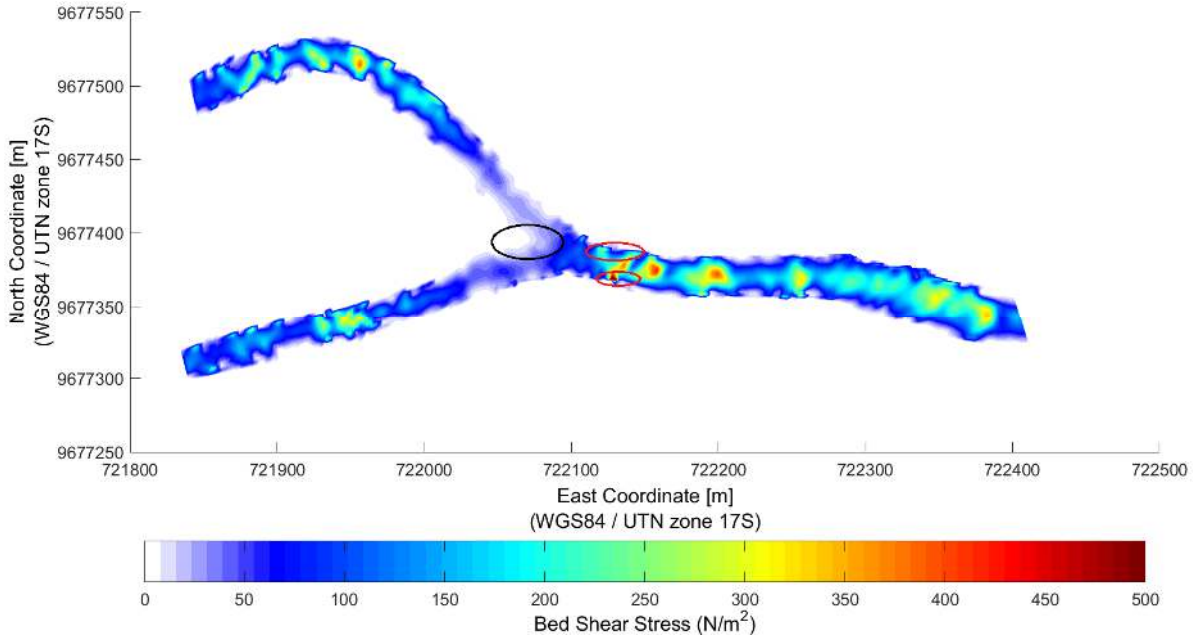

Figure 7 has seen that the zone of shear, mixing, and flow acceleration coincides with the values of the highest shear stress on the bottom of the channel. Special attention needs to be paid to the shear stresses produced near the banks since in these areas the flow heights are lower. Therefore, the erosive processes will have a greater impact on the solid boundaries of the flow.

The partial differential equations are formulated based on orthogonal curvilinear coordinates. Delft3D-Flow supports two grid systems in the vertical direction: σ model and Z-model. In the σ grid system, layers are bounded by two σ planes following the free surface and the bottom topography. A model in σ coordinates can provide a smooth topography demonstration because it is boundary fitted. However, in some cases where stratified flow occurs over a steep topography, σ grid may not have enough resolution. In the σ coordinate system, it is assumed that the vertical accelerations are much smaller than the gravitational acceleration, and thus, can be neglected. For cases in which this assumption is not valid, Delft3D-Flow can be extended with a nonhydrostatic pressure model that applies a Z grid system. Considering the uncertainties that may arise in both field measurements and modelling, the 3D hydrostatic Delft3D model was capable of producing the flow structures of the natural river bend with reasonable accuracy. Several reasons could be responsible for the discrepancies between the nonhydrostatic results and the measurements, including the errors that might have arisen due

to the pressure correction techniques, programming errors, and nonconservancy of the nonhydrostatic module (Parsapour-Moghaddam and Rennie, 2017).

4. Conclusions

The Delft3D three-dimensional hydrodynamic model was applied to evaluate the hydraulic characteristics of a mountain river confluence within the urban area of the city of Cuenca. Typical zones of a confluence were identified: stagnation, acceleration, mixing, recirculation, shear, and reestablishment of flow on the results of the water height and velocity averaged over the vertical and bottom shear stresses.

The flow heights are in the same order as the values observed in the hydrological stations considered to determine the flows contributed by the Yanuncay and Tarqui rivers. To evaluate the degree of accuracy in the numerical results obtained from the hydrodynamic simulation, the next step of the research is the characterization of hydrodynamic variables and solid boundaries in the confluence zone.

5. Acknowledgements

We acknowledge the financing of the Catholic University of Cuenca within the Research Projects (PICODS21-33) and Formative Research (PIFCV22-04) due to this collaboration it is possible to obtain the results presented and continue with the research of the tributaries of the Paute river basin. Special acknowledgments to the public companies of Ecuador ETAPA E.P. and CELEC E.P. for the information provided for the development of the research projects proposed by the Catholic University of Cuenca. The work presented falls under Sustainable Development Goal (SDG) 11: make cities more inclusive, safe, resilient and sustainable.

6. References

Ashmore, P.E., & Parker, G. (1983). Confluence scour in coarse braided streams. Water Resources Research, 19(2): 392-402. doi:10.1029/WR019i002p00392.

Behrangi, A., Borghei, S.M., & Daemi, A.R. (2004). Subcritical flow in open channel junction. In Proceeding of Hydraulics of dams and river structures conference, Tehran. Francis, London. pp. 392-400.

Best, J.L. (1986). The morphology of river channel confluences. Progress in Physical Geography 10(2), 157-174.

Best, J.L. (1987). Flow dynamics at river channel confluences: implications for sediment transport and bed morphology. In: Ethridge, F.G., Flores, R.M., Harvey, M.D. (Eds.), Recent Developments in Fluvial Sedimentology: Society of Economic Paleontologists and Mineralogists Special Publication No. 39. Society for Sedimentary Geology, Tulsa, OK, pp. 27–35.

Biron, P., Roy, A.G., & Best, J.L. 1996. The turbulent flow structure at concordant and discordant open channel confluences. Experiments in Fluids, 21(6): 437-444. doi:10.1007/BF00189046.

Cedillo-Galarza, J.S., Timbe-Castro, L.M., Samaniego-Alvarado, E.P., & Alvarado-Martínez, A.O. (2021). Efecto del refinamiento de la descripción de la rugosidad en una aproximación

2D para un río de montaña: un caso de estudio. La Granja: Revista de Ciencias de la Vida, 33(1):92-103. http://doi.org/10.17163/lgr.n33.2021.08.

CELEC E.P. (2023). Corporación Eléctrica del Ecuador, Unidad de Negocio CELECSUR [consultado 3 de abril 2023]. Disponible en: https://www.celec.gob.ec/celecsur/

Chow, V. T. (1959). Open-Channel Hydraulics, McGraw-Hill Book Company, Inc., Tokyo, Japan.

Constantinescu, G., Miyawaki, S., Rhoads, B., & Sukhodolov, A. (2014). Numerical evaluation of the effects of planform geometry and inflow conditions on flow, turbulence structure, and bed shear velocity at a stream confluence with a concordant bed. Journal of Geophysical Research: Earth Surface, 119, 2079–2097. doi:10.1002/2014JF003244.

Deltares. (2022). Simulation of multi-dimensional hydrodynamic flows and transport phenomena, including sediments [consultado 3 de abril 2023]. Delft3D-FLOW, User Manual. Disponible en: https://content.oss.deltares.nl/delft3d4/Delft3D-FLOW_User_Manual.pdf

Díaz-Lozada, J.M. (2019). Avances en la Cuantificación hidrológica y caracterización hidráulica del flujo en el sistema fluvial del Río Carcarañá utilizando ADCP. Tesis Doctoral. Facultad de Ciencias Exactas, Físicas y Naturales de la Universidad Nacional de Córdoba, Argentina.

ETAPA E.P., (2023). Red hidrometeorológica del cantón Cuenca [consultado 3 de abril 2023]. Disponible en: https://www.etapa.net.ec/informacion/gestion-ambiental/red-hidrometeorologica-del-canton-cuenca

Gurram, S.K., Karki, K.S., & Hager, W.H. (1997). Subcritical junction flow. Journal of Hydraulic Engineering, 123(5): 447-455. doi:10.1061/(ASCE)0733-9429(1997)123:5(447).

Gyssels, P., Baldissone, M., Hillman, G., Rodriguez, A., Bosc, J., Corral, M., Pagot, M., Brea, D., Spalletti, P., & Farias, H.D. (2013). Aplicaciones del modelo numérico DELFT3D a diferentes problemas hidrosedimentológicos en casos Argentinos [consultado 3 de abril 2023]. Mecánica Computacional Vol XXXII, 2757-2777, Disponible en: https://cimec.org.ar/ojs/index.php/mc/article/view/4517

Hager, W. H. (1989). Transitional flow in channel junctions. Journal of Hydraulic Engineering, 115(2): 243–259.

Huang, J., Weber, L.J., & Lai, Y.G. (2002). Three-Dimensional Numerical Study of Flows in Open-Channel Junctions. Journal of Hydraulic Engineering, 128(3): 268–280. doi:10.1061/(ASCE)0733-9429(2002)128:3(268)

Ibrahim, M.M., & Abdel-Mageed, N.B. (2014). Effect of Bed Roughness on Flow Characteristics, International Journal of Academic Research Part A, 6(5), 169-178, doi: 10.7813/2075-4124.2014/6-5/A.24

INEC, (2023). Conozcamos Cuenca a través de sus cifras [consultado 3 de abril 2023]. Disponible en: https://www.ecuadorencifras.gob.ec/conozcamos-cuenca-a-traves-de-sus-

cifras/#:~:text=Cuenca%2C%20tambi%C3%A9n%20conocida%20como%20la,este%20cant%C3%B3n%20tenga%20636.996%20habitantes

Minaya-Maldonado, V.G. (2017). Ecohydrology of the Andes Páramo Region (1st ed.). CRC Press. https://doi.org/10.1201/9781315116044

Mosley, M.P., (1976). “An experimental study of channel confluences”. Journal of Geology 84(5), 535-562.

Parsapour-Moghaddam, P., & Rennie, C.D. (2017). Hydrostatic versus nonhydrostatic hydrodynamic modelling of secondary flow in a tortuously meandering river: Application of Delft3D. River Research and Applications, 33: 1400– 1410. https://doi.org/10.1002/rra.3214

Ramamurthy, A.S., & Zhu, W. (1997). Combining flow in 90 junction of rectangular conduit. Journal of Hydraulic Egineering, 123(11): 1012-1019. doi:10.1061/(ASCE)0733-9429(1997)123:11(1012).

Rhoads, B. L., & Sukhodolov A. (2008). Lateral momentum flux and the spatial evolution of flow within a confluence mixing interface. Water Resources Research. Vol. 44.

SIGTIERRAS. (2023). Sistema Nacional de Información de Tierras Rurales e Infraestructura Tecnológica [consultado 3 de abril 2023]. Disponible en: http://www.sigtierras.gob.ec/

Shaheed, R., Mohammadian, A., & Yan, X. (2022). Numerical Simulation of Turbulent Flow in Bends and Confluences Considering Free Surface Changes Using the Volume of Fluid Method. Water, 14, 1307. https://doi.org/10.3390/w14081307

Shaheed, R., Mohammadian, A., & Yan, X. (2022). Numerical Simulation of Turbulent Flow in Bends and Confluences Considering Free Surface Changes Using the Volume of Fluid Method. Water, 14, 1307. https://doi.org/10.3390/w14081307

Shakibainia, A, Tabatabai M.R.M, & Zarrati A.R. (2010). Three-dimensional numerical study of flow structure in channel confluences. Canadian Journal of Civil Engineering. 37(5): 772-781. https://doi.org/10.1139/L10-016

Stelling, G. (1984). On the Construction of Computational Methods for Shallow Water Flow Problems, Ph.D. Thesis, Rijkswaterstaat Communication Series No. 35, Rijkswaterstaat, The Hague.

Taylor, E.H. (1944). Flow characteristics at rectangular open-channel junctions. Trans. Am. Soc. Civ. Eng., 109, 893–902.

Thanh, M.D., Kimura, I., Shimizu, Y., & Hosoda, T. (2010). Numerical simulation of flow at an open-channel confluence using depth-averaged 2D models with effects of secondary currents. Journal of Applied Mechanics Vol.13, pp.769-780.

Uittenbogaard, R.E., van-Kester, J. A. T. M., & Stelling, G. S. (1992). Implementation of three turbulence models in 3D-TRISULA for rectangular grids. Tech. Rep. Z81, WL | Delft Hydraulics, Delft, The Netherlands.

Vuille, M. (2013). Climate change and water resources in the tropical Andes. Inter-American Development Bank, Environmental Safeguards Unit, TECHNICAL NOTE No. IDB-TN-515.